

A Multivariate Cumulative Sum Method for Continuous Damage Monitoring with Lamb-wave Sensors

Spandan Mishra¹, O. Arda Vanli², and Chiwoo Park³

^{1,2,3} *Department of Industrial and Manufacturing Engineering,
Florida A&M University, Florida State University,
Tallahassee, FL 32310-6046, USA*

sm11ax@my.fsu.edu

oavanli@eng.fsu.edu

cpark5@fsu.edu

ABSTRACT

This paper proposes a new damage monitoring method based on a multivariate cumulative sum test statistic applied to Lamb-wave sensing data for health monitoring in composites. The CUSUM monitoring method applied to the features extracted with Principal Components Analysis was studied to improve robustness of detection and sensitivity to small damages. The method is illustrated with measured sensor data from fatigue loading and impact tests of carbon fiber materials and the performance of the proposed CUSUM approach was compared with existing Mahalanobis distance based monitoring techniques commonly applied in the health monitoring literature. It was shown that the CUSUM approach can significantly improve the misdetection rate for monitoring gradually developing damages.

Keywords: Structural Health Monitoring, Principal Components Analysis, Multivariate Cumulative Sum, Hotellings T^2 .

1. INTRODUCTION

Guided-wave structural health monitoring (SHM) is becoming increasingly popular for monitoring large structures with sparsely distributed sensors. Active sensor and actuator piezoelectric patches permanently attached or embedded in the structure are used to actively interrogate structural integrity by imparting elastic waves and measuring the resulting structural response (Raghavan & Cesnik, 2007). In contrast to metallic materials, composite materials present additional challenges in guided-wave health monitoring due to their anisotropic properties and complex failure characteristics. Therefore accurate and timely damage detection methods are crucial for reliable health monitoring of composites.

Spandan Mishra et al. This is an open-access article distributed under the terms of the Creative Commons Attribution 3.0 United States License, which permits unrestricted use, distribution, and reproduction in any medium, provided the original author and source are credited.

Gradual degradation is a commonly occurring phenomena in many engineering problems, for example due to cumulative crack growth (Bogdanoff & Kozin, 1985) and wear and fatigue (Gertsbackh & Kordonskiy, 1969). Load-carrying composite structures operating under tensile, fatigue or impact loading or corrosive environments develop damages during service, including matrix cracks, debonding and delamination. These damages are usually invisible to surface inspection and they do not immediately result in failure. However, it is important to continuously monitor the integrity of the structure and detect these damages early and prevent them from exceeding critical size and resulting in catastrophic failure. Detection of small damages is thus important to ensure that the structure safely operates before the damages reach critical size and make repairs only when needed, a common goal in condition-based maintenance (Wang, 2000). The objective of this article is to develop a new statistical control chart for detecting small changes based on readings of a guided-wave sensor.

The majority of the existing SHM methods utilize either univariate outlier analysis or multivariate Mahalanobis distance based approaches. Worden et al. (2000) which are very good for detecting relatively large damages but may be ineffective for continuous monitoring of slowly developing damages. This paper proposes a new multivariate cumulative sum (CUSUM) damage monitoring method with Lamb-wave sensors that improves detection time and misdetection rates for fatigue loading conditions. Fatigue cycles are accumulative in nature wherein each cycle causes very small change in the property of the structure. These changes should be accurately tracked to prevent any catastrophic failure of the structure. CUSUM enables us to keep track of these small changes by continuously monitoring. A principal component analysis (PCA) is applied to raw sensor signals to extract important features which are then used in the monitoring scheme. The effectiveness of the approach is illustrated on fatigue loading

and impact damage cases with Lamb-wave sensing data. It is shown that the multivariate CUSUM can significantly improve monitoring accuracy of Hotelling's T^2 when the structure being monitored is undergoing fatigue loading.

The rest of the paper is organized as follows. Section 2 reviews relevant literature in structural health monitoring and damage monitoring and detection. Section 3 shows the development of the proposed multivariate cumulative Sum for damage monitoring. Section 4 presents application of the method on measured Lamb-wave data and comparison to existing damage quantification approaches. Section 5 provides the concluding remarks of the paper.

2. REVIEW OF RELEVANT LITERATURE: GUIDED-WAVE SENSING AND STATISTICAL METHODS FOR DAMAGE MONITORING

Lamb-waves are elastic perturbations that propagate in a solid plate in two dimensions (Viktorov, 1967). The most commonly used transducers to excite Lamb-waves are embedded or surface-bonded piezoelectric sensors (Giurgiutiu, 2005). When operating as a transmitter they transform electrical energy into mechanical energy. Surface strains are generated when voltage is applied to the piezoelectric patch and it expands and contracts parallel to the surface. Similarly, when operating as a receiver they transform mechanical energy into electrical energy. Voltage is generated on the piezoelectric due to local stress and strain (Diamanti et al., 2004). Lamb-wave sensors operate either in pitch-catch or pulse-echo modes. In a pitch-catch configuration, the diagnostic signal emitted from the actuator travels across the damaged area while the sensor on the other side of area receives the signal. On the other hand, in a pulse-echo configuration the actuator and sensor are placed on the same side of the inspection area and the sensor receives the signal echoed from the damage (Kessler et al., 2002). A useful characteristic of a Lamb-wave is that whenever it reaches a region of discontinuity, a portion of the wave is reflected proportionally to the difference in the stiffness and density of the material. Analysis of the incident wave can therefore reveal useful information about the location and size of damage. In this paper we use a pitch-catch based actuator-sensor configuration (Ihn & Chang, 2004).

Feature extraction is an important data analysis step in Lamb-wave based damage monitoring. Features of the waveforms that are sensitive to the damages need to be identified and estimated from the raw sensor data. Damage detection then consists of comparing the features of waveforms from the damaged structure to those of the undamaged structure. Feature extraction is classified into model-based and signal-based methods. Model-based approaches use certain pre-established models to extract features from the signal while signal-based approaches extract features from the signal without applying any sort of deterministic model to the signal (Su et al., 2006).

The feature extraction process using Lamb-waves proposed in this paper falls into the second category (signal-based methods).

Pullin et al. (2008) have applied PCA on acoustic emission signals to differentiate fatigue crack propagation from background noise of a landing gear component. PCA is a dimensionality reduction technique that is often used to transform a high dimensional data-set into smaller-dimensional subspace. The authors have used first and second principal components (PC) of the sensor signal to separate fatigue source signal from the landing gear noise. Pavlopoulou et al. (2013) used nonlinear principal component analysis and principal curves for damage prognosis. Cross et al. (2012) proposed a method to filter out environmental variations in Lamb-wave sensors by projecting the data into its minor components so that the dimensions of the data that carry any dependence on environment factors can be discarded. Kessler & Agrawal (2007) applied PCs to Lamb-wave data to detect the presence, type and severity of various types of damage. PCs of the original sensor data vector that explain about 70% of the variability are used in a K -th nearest neighbor algorithm to classify the damage mode.

Statistical process control methods have been used extensively for variation reduction in manufacturing. The Shewhart control charts are employed as the main tool to detect shifts from an in-control statistical model and to make sure the process continues to operate in a stable manner (Montgomery, 2007). When multiple correlated quality characteristics are of interest then multivariate control charts should be used to simultaneously monitor all characteristics and detect deviations. Hotelling's T^2 is the multivariate counterpart of the Shewhart chart for monitoring the mean vector of a process (MacGregor & Kourti, 1995). While the Shewhart charts can detect large process upsets reasonably well, in order to better detect small shifts cumulative sum procedures, a set of sequential procedures based on likelihood ratios, are recommended (Woodall & Ncube, 1985). Cumulative sum utilizes the entire history of the observed data, in contrast to the Hotelling's T^2 or Shewhart charts which utilize only the current data point, and are therefore more sensitive to gradually developing small shifts in the signal mean. Multivariate cumulative sum methods have been proposed by Woodall & Ncube (1985), who used multiple univariate CUSUMs to test shifts in the mean of a multivariate normal, and by Crosier (1988), who used the accumulated deviations of vectors from the baseline and produce a quadratic form to find a scalar monitoring statistic. Pignatiello & Runger (1990) compared and outline the benefits of various multivariate CUSUM approaches.

Statistical process control techniques have been utilized in structural health monitoring by many authors. Sohn et al. (2000) used Shewhart \bar{X} charts to monitor coefficients of an auto-regressive time series model fitted to the measured vi-

bration time histories from an undamaged structure. Control limits of the charts are determined to detect deviations of the coefficients from the initial structures for damage detection. For monitoring multiple features extracted from sensor signals, Worden et al. (2000) and Sohn et al. (2000) extended the univariate control charts to multivariate charts by using a Mahalanobis distance to quantify the distance between potential outlier vector and the in control sample mean vector, a measure similar to the Hotelling T^2 statistic. Mujica et al. (2010) used PCA in conjunction with a T^2 statistic to extract features from multi-sensory arrangement on a turbine blade to detect the variation due to damages in the subspace of the dominant principal components that are greater than what can be explained by the common cause variations. Deraemaeker et al. (2008) applied factor analysis to subdue the effects of environmental fluctuation on data and used multivariate control charts for damage detection. Kullaa (2003) used missing data model to eliminate environmental and operational variances and Hotelling T^2 chart to monitor changes in modal parameters and to detect the possible damage in the structure.

3. PROPOSED METHODOLOGY-MULTIVARIATE CUMULATIVE SUM MONITORING WITH PRINCIPLE COMPONENTS

Lamb-wave sensor data is a high dimensional vector (on the order of thousands, depending on the sampling frequency) and some form of dimension reduction is required to practically monitor fewer variables and to achieve robust and repeatable detection performance. Principle component Analysis (PCA) is a popular multivariate statistical analysis method for dimension reduction in process monitoring and fault diagnosis applications (Jackson, 2005). The method transforms a set of correlated variables to a smaller number of uncorrelated new variables. The original vector of variables $\mathbf{x} = (x_1, \dots, x_p)$ is projected into a vector of new variables $\mathbf{z} = (z_1, \dots, z_r)$ called the principal components. In the new coordinate system, z_1 is a linear combination of the original variables x_1, \dots, x_p and explains the maximum possible variance, z_2 , another linear combination, is orthogonal to z_1 and explains most of the remaining variance, and so on. It can be seen that if the original set of p variables are actually a linear combination of r new variables, then the first r principal components will be sufficient to explain all the variance and remaining $p - r$ principal components are very small.

The monitored area of the structure is assumed to incur some damage when the sensor data vector deviates significantly from a baseline (no damage) condition. The baseline condition is represented by collecting a set of N observations with the sensor under the no damage condition and the data is given in a $p \times N$ matrix $\mathbf{X} = [\mathbf{x}_1, \mathbf{x}_2, \dots, \mathbf{x}_N]$ in which each $p \times 1$ column vector \mathbf{x}_j represent an observation $j = 1, 2, \dots, N$. In practice the sensor data must be scaled in some meaningful way to account for differences in the measure-

ment units of the variables. A typical approach is scaling so that all variables have zero mean and unit variance as $x_{ij} = (\tilde{x}_{ij} - \mu_i)/\sigma_i$, where $(i = 1, 2, \dots, p, j = 1, 2, \dots, N)$ and \tilde{x}_{ij} is the original data, μ_i and σ_i are the sample mean and standard deviations along the i -th dimension. The covariance matrix of the sensor data $\mathbf{C} = 1/(n - 1)\mathbf{X}\mathbf{X}^T$ is decomposed, using singular value decomposition, as $\mathbf{C} = \mathbf{V}\mathbf{D}\mathbf{V}^T$ into an orthogonal eigenvector matrix $\mathbf{V} = [\mathbf{v}_1 \ \mathbf{v}_2 \ \dots \ \mathbf{v}_p]$ and a diagonal eigenvalue matrix $\mathbf{D} = \text{diag}(\lambda_1, \lambda_2, \dots, \lambda_p)$, both matrices are of size $p \times p$ and the eigenvalues are in descending order $\lambda_1 > \lambda_2 > \dots > \lambda_p$. It can be seen that the i -th principal component is the linear combination:

$$z_i = \mathbf{v}_i^T \mathbf{x} = v_{i1}x_1 + v_{i2}x_2 + \dots + v_{ip}x_p \quad (1)$$

in which \mathbf{v}_i is the i -th column of the \mathbf{V} matrix ($i = 1, \dots, r$) also called the i -th the principal component *loading vector* or *eigenvector*. Principal component *scores* of an observation vector are the inner products of the observation vector with principle component loading vectors. For example for the j -th ($j = 1, \dots, N$) sensor data \mathbf{x}_j the score for the i -th ($i = 1, \dots, r$) principal component (PC) is $z_{ij} = \mathbf{v}_i^T \mathbf{x}_j$. In practice the first r principal components will be sufficient to represent most variability of the original data, thus the eigenvectors associated with the eigenvalues $\lambda_{r+1}, \dots, \lambda_p$ are discarded and a reduced eigenvector matrix \mathbf{V} of size $p \times r$ is formed. The transformation to the principal component scores is obtained through the matrix multiplication $\mathbf{z} = \mathbf{V}^T \mathbf{x}$ in which \mathbf{x} is the vector of raw sensor data of size $p \times 1$ and \mathbf{z} be the $r \times 1$ vector of principle components in the reduced dimension.

To detect a damage with a given confidence level, the PCA method is followed by a decision making procedure based on Hotelling's T^2 , a statistic for testing differences between mean values of two data groups (MacGregor & Kourti, 1995). The sensor data collected from the baseline (undamaged) structure is used to establish an upper control limit (UCL) for the T^2 statistic under the $100(1 - \alpha)\%$ confidence level, which enables one to control the false alarm probability (the probability that an alarm is generated when in fact there is no damage) to α . It is assumed that under the baseline (no damage) condition the raw sensor data \mathbf{x} follows a p -dimensional vector Normal distribution with mean vector $\boldsymbol{\mu}_0$ and covariance matrix \mathbf{C} . To determine when the sensor data indicates damage, deviations from baseline is monitored by calculating the Hotelling T^2 statistic, defined as:

$$T^2 = (\mathbf{x} - \boldsymbol{\mu}_0)^T \mathbf{C}^{-1} (\mathbf{x} - \boldsymbol{\mu}_0) = \sum_{i=1}^r \frac{(\mathbf{v}_i^T \mathbf{x})^2}{\lambda_i} \quad (2)$$

in which, the term after the first equality sign represents the test statistic in terms of the original sensor vector \mathbf{x} and the term after the second equality sign is the representation based on the r principal components (MacGregor & Kourti, 1995).

Under the hypothesis of no damage, the T^2 statistic follows an F distribution and to control the false alarm rate at α the upper control limit (UCL) of the monitoring statistic is set at

$$UCL_F = \frac{(N-1)(N+1)r}{N(N-r)} F_\alpha(r, N-r) \quad (3)$$

where N is the sample size, $F_\alpha(r, N-r)$ is the upper $100\alpha\%$ point of the F distribution with r and $N-r$ degrees of freedom. If both r and N are large, then the estimation errors of the parameters are assumed negligible and a χ^2 distribution can be used for the hypothesis of no change. The UCL is estimated as upper $100\alpha\%$ point of a χ^2 distribution with r degrees of freedom (Montgomery, 2007, p. 371),

$$UCL_{\chi^2} = \chi^2(\alpha, r). \quad (4)$$

As soon as the test statistic exceeds the control limit, i.e., $T^2 > UCL$, an alarm is given indicating a damage has initiated. Otherwise, i.e., $T^2 \leq UCL$, it is assumed that the structure still operates in the baseline no damage condition.

Many authors who have studied Hotelling's T^2 control charts have concluded that the chart is quite effective for detecting large and sustained shifts (three standard deviations or larger from baseline) however, it may take a long time to signal an alarm for relatively small or gradually developing shifts (on the order of one or two standard deviations (Lowry & Montgomery, 1995). This presents a limitation for structural health monitoring applications, where it is important to be able to detect cracks or delaminations early on, from the onset, to be able to continuously monitor as they grow and react on time by scheduling repair or replacement, if the growth becomes rapid.

In this paper we propose a new multivariate cumulative sum (CUSUM) approach for detecting and monitoring small damages with Lamb-wave sensors. In order to detect small shifts a commonly used approach is to use a cumulative sum statistic which utilizes not only the most recent sensor measurement but also the past observations as well in order to more quickly expose slowly accumulating changes (Woodall & Ncube, 1985). A principal component analysis is conducted on the raw sensor data to find the feature vector on which the CUSUM chart operates. We follow the formulation studied by Pignatiello & Runger (1990) in which a cumulative multivariate difference vector between the observed PC score vector \mathbf{z} and the expected (under baseline) scores at time t is defined as:

$$\mathbf{s}_t = \sum_{i=t-n_t+1}^t (\mathbf{z}_i - \boldsymbol{\mu}_{z0}) \quad (5)$$

where $\boldsymbol{\mu}_{z0} = \mathbf{0}$ for baseline PC scores. The cumulative sum (CUSUM) statistic to be monitored is

$$MC_t = \max\{0, \|\mathbf{s}_t\| - kn_t\} \quad (6)$$

in which the norm of \mathbf{s}_t is found as $\|\mathbf{s}_t\| = (\mathbf{s}_t^T \mathbf{D}^{-1} \mathbf{s}_t)^{1/2}$ with \mathbf{D} being the matrix of eigenvalues and the summation is found using n_t , the number of measurements since the last renewal (zero value) of the CUSUM, defined as:

$$n_t = \begin{cases} n_{t-1} + 1 & \text{for } MC_{t-1} > 0 \\ 1 & \text{otherwise.} \end{cases} \quad (7)$$

The CUSUM statistic accumulates differences that are larger than k , which is a chart parameter that needs to be specified by the user, usually taken as one half of the desired change in the mean vector we want to make the chart sensitive for. If the CUSUM statistic exceeds the upper threshold h of the chart, that is, if $MC_{t-1} > h$, then an out of control alarm is signaled. There is no closed form expression to the reference distribution for the statistic, therefore the threshold to achieve a desired false alarm rate under the hypothesis of no damage is found by simulation (Pignatiello & Runger, 1990). In our study, we conduct Monte Carlo simulation, to generate replicated realizations of the in control process (under the hypothesis of no damage) with increasing threshold h values to find the value that gives an average run length (the average time to signal an alarm) of 200 samples (Lowry & Montgomery, 1995). This value, which corresponds to the false alarm probability of $\alpha = 0.005$, is a commonly used value to tune control charts (Montgomery, 2007).

4. APPLICATION OF THE PROPOSED APPROACH

In this section we illustrate the application of the proposed damage monitoring method under two different damage conditions. Both cases involve Lamb-wave condition data. The first data set, available from public domain, corresponds to fatigue loading and contains sensor data under cycled loading until failure for multiple specimens. The second data set corresponds to impact tests that we have conducted for one specimen.

4.1. Fatigue tests:

The fatigue data set provided by the Prognostic Center of Excellence of NASA Ames Research Center (Saxena et al., 2015) is used in this study. The data corresponds to Lamb-wave sensor measurements from carbon fiber composite coupons during tension-tension fatigue tests. Two sets of six piezoelectric sensors were attached on both ends of a dogbone shaped coupon of size 152.4 mm by 254 mm. A notch (of size 5.08 mm by 19.05 mm) is introduced to induce stress concentration and accelerate delamination growth at this site. Different layup configurations were presented in the dataset: Layup 1: $[0_2/90_4]$, Layup 2: $[0/90_2/45/-45/90]$, and Layup 3: $[90_2/45/-45]_2$. We used the data for the first layup config-

uration. X-ray images taken from the samples show that after about 10 to 100 cycles delamination damage starts to develop in the specimens. Data from three such coupons for the first layup (labelled as L1S11, L1S12 and L1S19 in the data set) were used to illustrate our monitoring methods. Two X-ray images for the first coupon are shown in Figure 1.

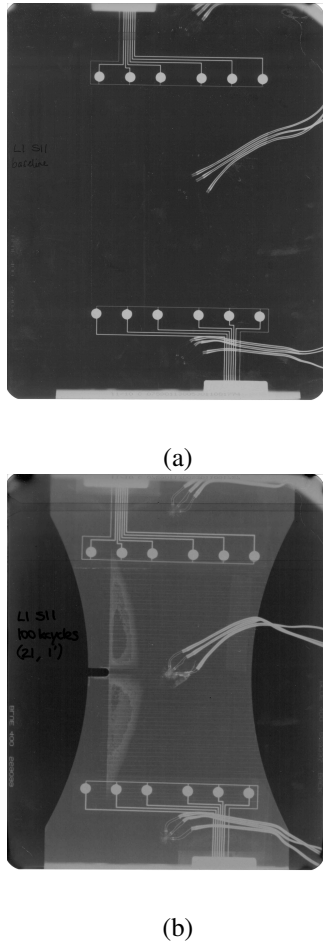


Figure 1. (a) X-ray image of the first coupon (L1S11) under baseline condition. (b) X-ray image of the first coupon (L1S11) after 100K cycles of fatigue loading, delamination can be seen as light gray colored region centered around the notch (Saxena et al., 2015). The sensors at the top are numbered 1 to 6 from right to left and the sensors at the bottom are numbered 7 to 12 from left to right.

Lamb-wave data are collected both before the test has started and after fatigue loading was applied. We considered the path between actuator 1 and sensor 7 and the interrogation frequency of 200 kHz. We considered this path in this study because it is the diagonal path, covering the largest area, between the two sensor patches among all possible pairs of actuators and sensors and we assumed that it represents a worst case scenario. Figure 2 shows the Lamb-wave signals measured at baseline and fatigue loading conditions from the first

coupon. A sampling rate of 1.2 MHz is used to acquire sensor signals for 1667 microseconds long time series. This resulted in 2000 data points for each sensor measurement, thus, \mathbf{x} is a $p = 2000$ dimensional vector. Baseline state corresponds to from 0 to 5 cycles and the fatigue damage corresponds to from 10 cycles to 10 million cycles. Under the baseline, there are 14 measurement points for coupon 1, 13 measurement points for coupon 2 and 10 measurement points for coupon 3. Under the fatigue loading, there are 24 measurement points for coupons 1 and 2, and 26 measurement points for coupon 3. Figure 1 corresponds to the measurement of the first coupon at baseline (top) and after 100K cycles (bottom).

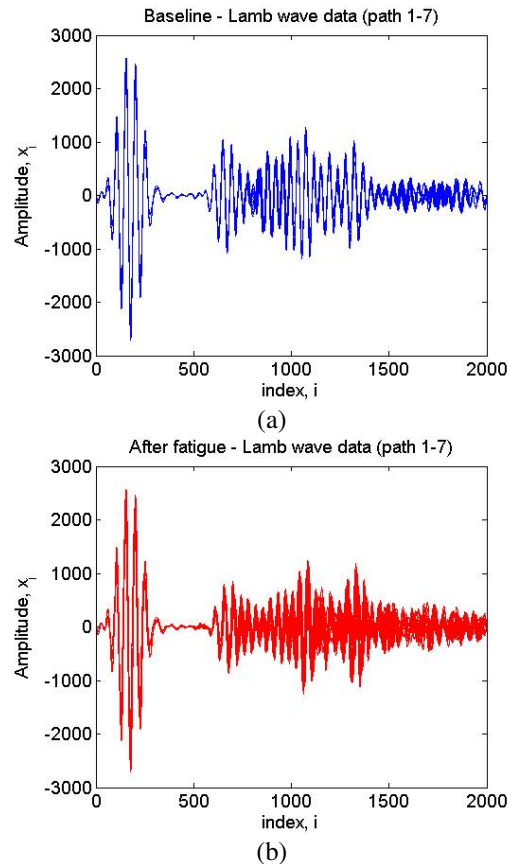


Figure 2. Lamb-wave sensor data for fatigue tests for the first coupon (a) Data before loading has been applied. 14 sensor trajectories are shown. (b) Data after fatigue loading has been applied. 24 sensor trajectories were collected.

We find the principle component loading vectors $\mathbf{v}_1, \dots, \mathbf{v}_p$ of the 14×2000 baseline data matrix \mathbf{X} . Figure 3a shows the proportion of variance explained by additional principal components, indicating that $r = 5$ principle components is sufficient to explain about 97% of the variation and is selected as the reduced dimension representation of the sensor data. Figure 3b gives the histogram of the T^2 values found from the scores of the 5 principle components of the baseline data

using Equation 2. The superimposed curve corresponds to

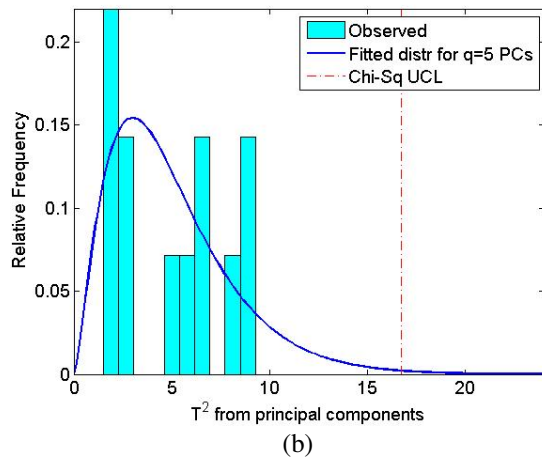
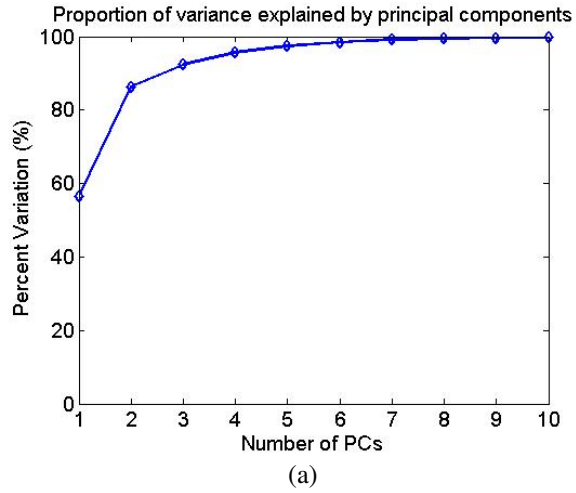


Figure 3. (a) Cumulative variance explained by additional principal components. (b) Histogram of the T^2 values found from the PC scores of baseline data and the expected χ^2 distribution under no damage is superimposed.

the F distribution that the test statistic is expected to follow, which shows a reasonable fit to the data. The UCL for the T^2 control chart is found as the 99.5% percent point (vertical red line) of the distribution which results in 0.005 false alarm rate (the area under the curve to the right of the UCL).

Figure 4 shows the principle component scores of the five principal components computed both from the baseline and fatigue loading conditions for the first coupon. Figures 5, 6 and 7 show the T^2 and the multivariate CUSUM statistics computed using the PC scores for all three coupons.

All charts are obtained by applying the principal component analysis (also 5 PC's are used) on the Lamb-wave data from the tests. The vertical line delineates the results determined from the baseline and fatigue loading conditions. For the T^2 charts, the horizontal red line is the upper control limit esti-

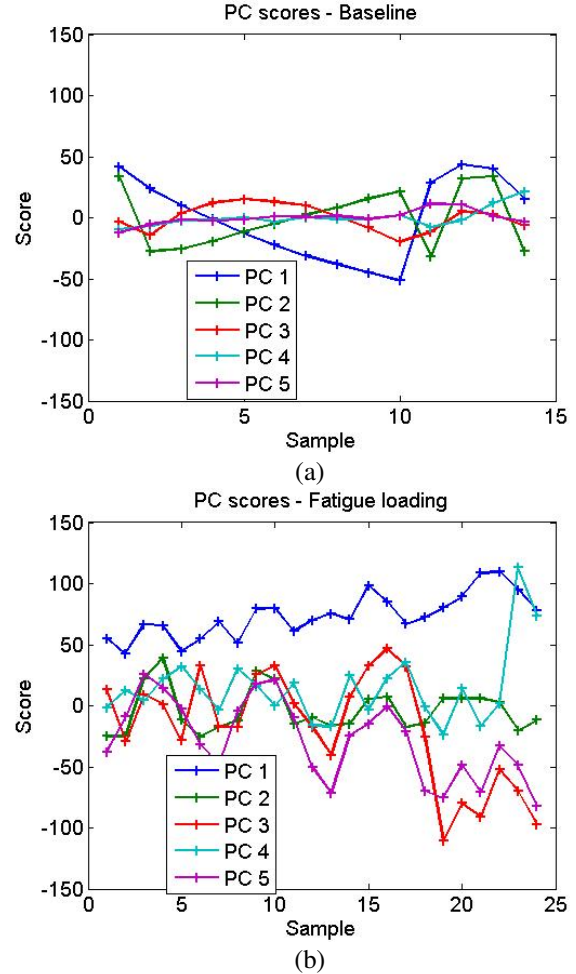


Figure 4. The first 5 Principal component scores of the raw signal. (a) Principal components of baseline signal. (b) Principal components of signal under fatigue loadings.

mated using the F -distribution and the horizontal black line is the upper control limit estimated using the χ^2 -distribution. The control limits are: $UCL_F = 57.81$ found using Equation 3 and F distribution with $N = 14$ and $r = 5$ and $UCL_{\chi^2} = 16.75$ using Equation 4 and χ^2 distribution with $\alpha = 0.005$ and $r = 5$. As it can be seen, to maintain the false alarm rate while accounting for parameter estimation errors, the chart calls for widening of the control limits. The T^2 statistic is obtained from Equation 2. For the CUSUM chart the difference vector s_t was found from Equation 5 and the cumulative sum statistic MC_t is found by applying Equation 6, in which the subscript t denotes the sample or measurement number. The upper control limit (horizontal red line) is found as $h = 6.64$ by running 1000 Monte Carlo simulations. For the CUSUM chart we set $k = 0.5$ to make the chart sensitive to one half of one standard deviation shifts.

It can be seen that for all three coupons, the charts do not signal any false alarms under the no damage condition: none

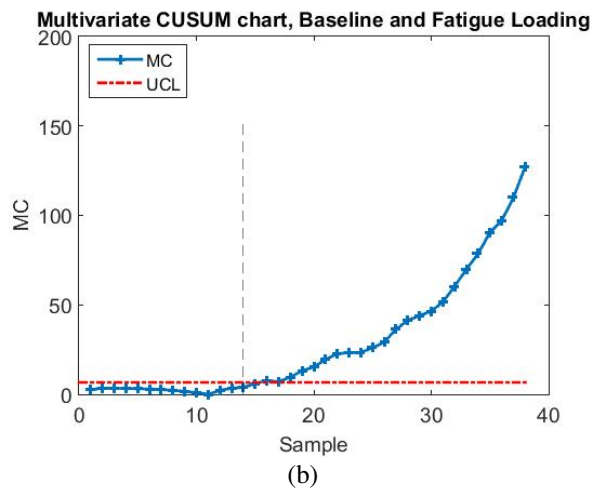
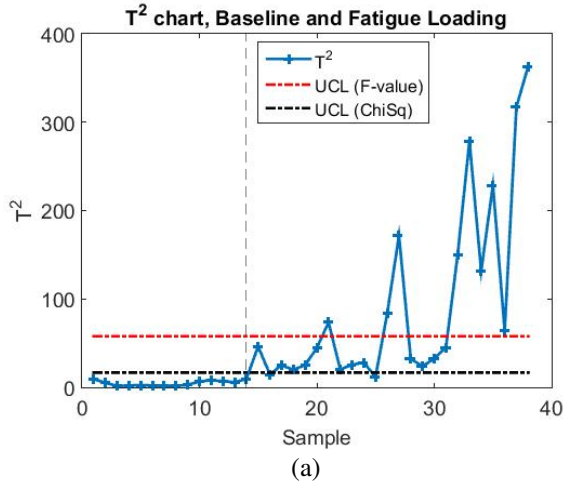


Figure 5. Control charts plotted from the principal component scores (coupon 1). (a) Hotelling T^2 chart obtained from the principal component scores, horizontal red line represents upper control limit (UCL) estimated using F-distribution. Horizontal black line represents UCL estimated using χ^2 distribution. Vertical black line separates the results for baseline and fatigue loading conditions. (b) Multivariate CUSUM, the horizontal red line represents upper control limit obtained for average runlength of 200.

of the test statistics plotted in Figures 5, 6 and 7 to the left of the vertical line crosses the horizontal red line and black line. For the first coupon (Figure 5a) the T^2 chart estimated using the F -distribution correctly detects the fatigue damage only at the sample 21. It misses all the damage states from sample 15 to 20. Furthermore, after correctly detecting damage at sample 21, it misses 4 consecutive damage conditions namely, samples 22, 23, 24 and 25. The T^2 chart estimated using χ^2 distribution has slightly better performance: it signals the alarm correctly at sample 15, however misses 2 conditions later on for samples 16 and 25. On the other hand, the CUSUM statistic plotted in Figure 5b signals the alarm correctly right after sample 15, and from that point onward it

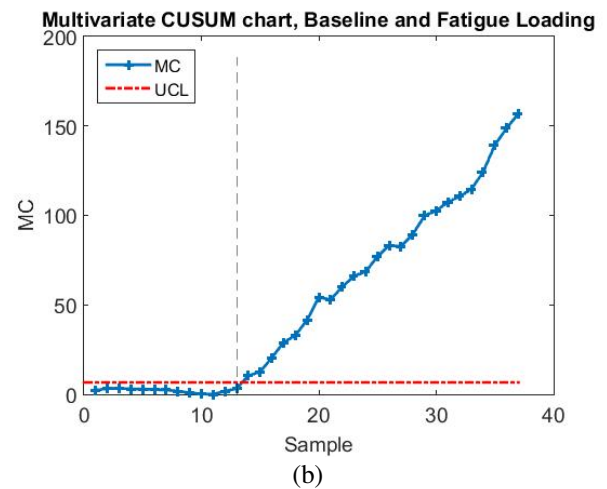
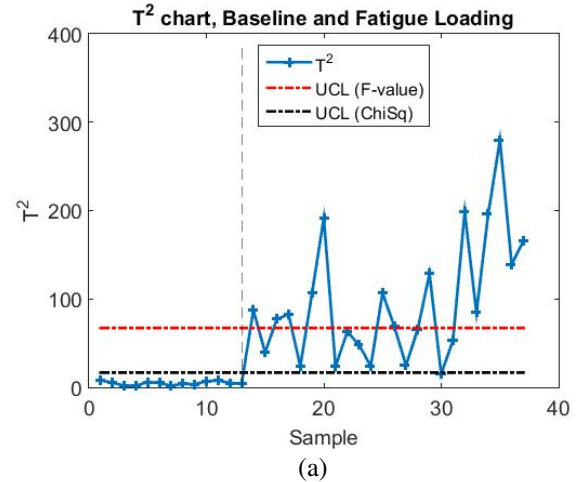


Figure 6. Control charts plotted from the principal component scores (coupon 2). (a) Hotelling T^2 chart obtained from the principal component scores, horizontal red line represents upper control limit (UCL) estimated using F-distribution. Horizontal black line represents UCL estimated using χ^2 distribution. Vertical black line separates the results for baseline and impact loading conditions. (b) Multivariate CUSUM, the horizontal red line represents upper control limit obtained for average runlength of 200.

has no misdetections. For the second coupon (Figure 6) both the T^2 and CUSUM charts detect the shift on time at sample 14. However, T^2 estimated using F-distribution has 10 misdetections later on at samples 15, 18, 21, 22, 23, 24, 27, 28, 30 and 31, T^2 estimated using χ^2 distribution performs slightly better and has 1 misdetection later on at sample 30. The CUSUM statistic consistently increases with no misdetections. The third coupon (Figure 7) was more challenging for all methods. We see that the T^2 from F -distribution is not able to detect the damage (sample 11) at all (Figure 7a, horizontal red line). T^2 estimated using χ^2 distribution (horizontal black line) sounds the first alarm at sample 17 (it takes 7 samples to detect the damage) and only samples 17, 19 and

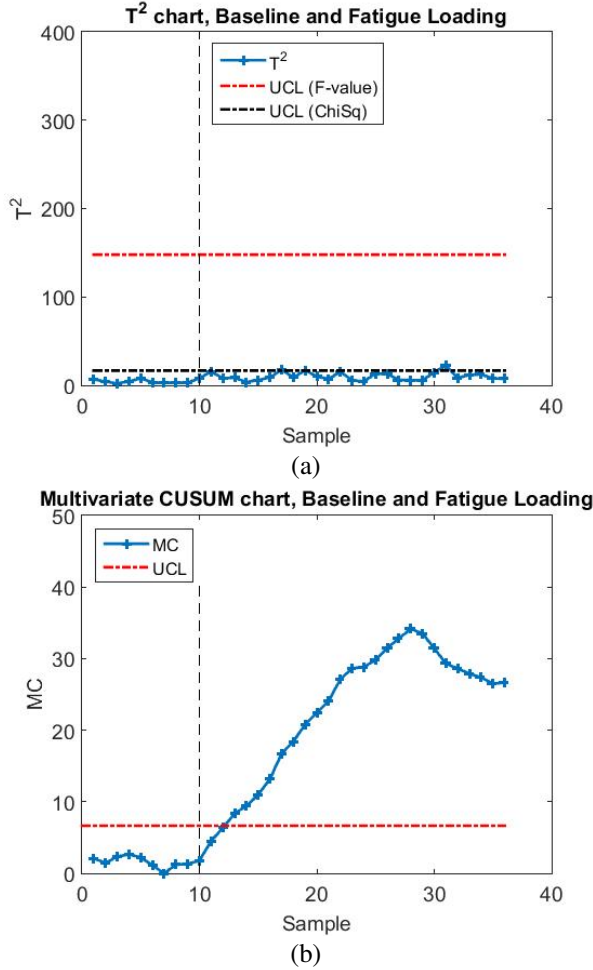


Figure 7. Control charts plotted from the principal component scores (coupon 3). (a) Hotelling T^2 chart obtained from the principal component scores, horizontal red line represents upper control limit (UCL) estimated using F -distribution. Horizontal black line represents UCL estimated using χ^2 distribution. Vertical black line separates the results for baseline and fatigue loading conditions. (b) Multivariate CUSUM, the horizontal red line represents upper control limit obtained for average runlength of 200.

31 out of the 26 damage samples were detected. By contrast, the CUSUM chart (Figure 7b) signals the first alarm at sample 13 (it takes only 3 samples to detect the damage) and it correctly classifies all subsequent 23 samples as damaged. We summarized these detection results in Table 1. Overall, the

Table 1. Mis-detection rates for the CUSUM and T^2 charts from fatigue loading tests

Cpn	CUSUM	T^2 (Use F)	T^2 (Use χ^2)
1	1 of 24 (4.2%)	14 of 24 (58.3%)	2 of 24 (8.3%)
2	0 of 24 (0.0%)	10 of 24 (41.67%)	1 of 24 (4.2%)
3	3 of 26 (7.7%)	26 of 26 (100%)	23 of 26 (88.5%)

CUSUM chart signals alarms much faster (which results in a lower mis-detection rate) than the traditional T^2 charts under small fatigue damages. No false alarms have been observed with either of the charts. The summary of mis-detection rates (smaller the better), given in Table 1, shows that T^2 chart with χ^2 control limits perform better than the F distribution, however, the CUSUM chart consistently outperforms the T^2 charts. We note that the coupons have identical layouts and are expected to have similar damage propagation behavior, however, there are some differences in the detection performance, especially for the T^2 chart. We note that the T^2 chart estimated using χ^2 distribution tightens the control limits found by the F distribution as it neglects the parameter estimation errors. In the three coupon cases we considered, this did not result in any false alarms (signaling a damage condition when in fact there is no damage) and improved the detection rate. However, in practice one has to be cautious about using too tight control limits as it may result in excessive false alarms.

4.2. Impact tests:

In this section we present an experimental study to monitor impact damage with the proposed method. A three-ply carbon fiber polymer composite panel of size 68.58 cm \times 25.4 cm \times 0.0889 cm is used for the experiments. Two Lamb-wave sensors are surface mounted on the panel 66.04 cm apart in the length direction of the panel and mid-way from the width direction. A 12.90 cm² teflon sheet is inserted between first and second layer of carbon-fibre sheet halfway between the two sensors at the time of curing. The composite was cured with the teflon sheet in-between the fibers so that adhesion of layers is prevented and to concentrate impact stress. The teflon sheet helps to control the location and size of damage. Impact loading is generated by dropping a 2.99 kg weight on the same laminate from increasing heights. Every impact of the weight exerts higher force on the composite panel. The heights of the weight are 1 m, 1.49 m, 1.71 m, 1.89 m, and 2.01 m. In order to verify the delamination damage, we inspected the panel before and after the impact tests using ultrasound C-scan. Figure 8 shows the C-scan image of the panel after the last tests and the Lamb-wave measurements from the tests (baseline and impacts).

We collected $N = 11$ measurements from the pristine panel before generating any impacts to represent the baseline (no damage) condition. The piezoelectric excitation frequency of 400 KHz was determined from a preliminary experiment (in which the specimen is scanned by frequencies ranging from 50 KHz to 500 KHz) to minimize the amount of dispersion in the actuator signal group velocities. The sampling rate of the 12 MHz is used to acquire the signals for 500 microseconds long time series, which resulted in 6000 data points for each sensor measurement, that is, \mathbf{x} is a 6000×1 vector.

From the 11×6000 baseline data matrix \mathbf{X} we found that 6

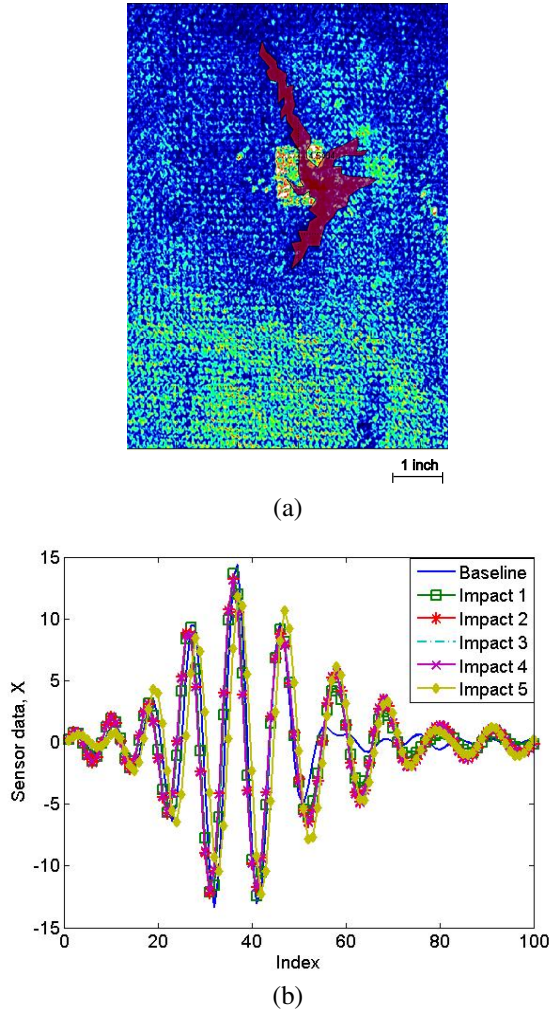


Figure 8. (a) C-scan image of the impacted laminate. The red highlighted region shows delaminated area (b) Lamb-wave data from impact tests and the average of the data from baseline condition. The impact test data are individual sensor readings from 5 tests. The baseline data is the average of 11 sensor readings.

principal components explain about 85.27% of the variability and used as the reduced dimensional representation of the original data. The loading vectors for the baseline data and the data for the 5 impacts are shown in Figure 9. The magnitudes of all principal components are smaller under the baseline condition than those after impacts, illustrating the deviation that occurs from the baseline in multiple dimensions under the impact damage.

Figure 10 shows the control charts found from the principle component scores. The UCL for the T^2 control chart estimated using the F and χ^2 distributions for the significance level of 0.5% as 189.99 and 18.57, respectively.

For the multivariate cusum chart we used $k = 0.5$ and h

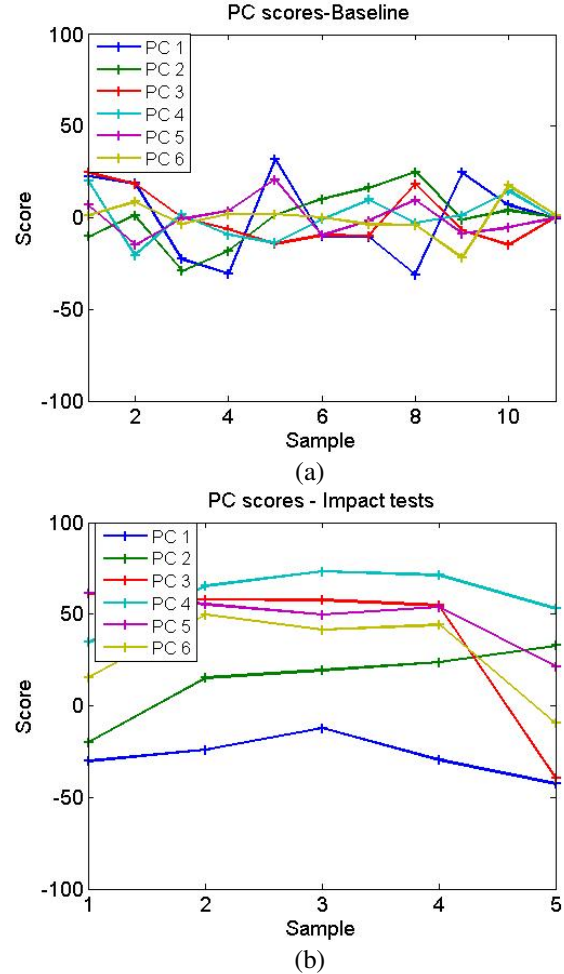


Figure 9. The first 6 Principle component scores for the impact tests. These principal components are used to find the test statistic values in the T^2 and CUSUM charts (a) Principal components from 11 baseline conditions and (b) Principal components from 5 impact tests.

was found to be 7.45 from 1000 Monte Carlo simulations for $r = 6$ dimensions. It can be seen in Figure 10 that the T^2 chart using the F -distribution (horizontal red line) is not able to detect any damages while the T^2 chart from the χ^2 distribution that does not account for estimation errors (horizontal black line) is able to detect all damaged samples 11, 12, 13, 14, and 15, correctly. By contrast, the proposed CUSUM approach is able to detect all but first damage sample. The fact that a CUSUM chart is relatively slow to the impact change compared to the T^2 chart is in agreement with the well known property that T^2 charts are more sensitive to isolated and large changes while CUSUM charts are more sensitive to small and gradual changes (Montgomery, 2007). The change in mechanical properties are more abrupt and large in impact loading conditions than fatigue loading conditions which produce gradual changes. We can see that the T^2 chart

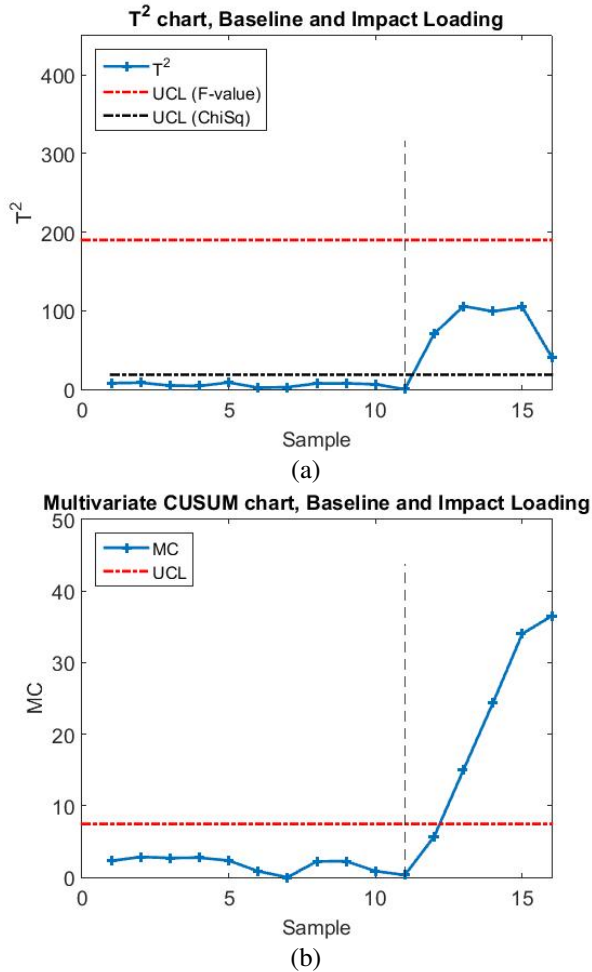


Figure 10. Control charts plotted from the principal component scores (impact sample). (a) Hotelling T^2 chart obtained from the principal component scores, horizontal red line represents upper control limit (UCL) estimated using F -distribution. Horizontal black line represents UCL estimated using χ^2 distribution. Vertical black line separates the results for baseline and fatigue loading conditions. (b) Multivariate CUSUM, the horizontal red line represents upper control limit obtained for average runlength of 200.

with χ^2 distribution that did not account for estimation errors performed somewhat better in detecting larger changes than CUSUM in the impact tests (T^2 chart with F -distribution was not able to detect any impact damages). By contrast, when the change is more gradual, as in the fatigue tests, CUSUM has a much higher detection accuracy than T^2 charts.

5. CONCLUSION

Guided-wave sensing based health monitoring has received increased interest in recent years due to the low cost implementation of these sensing systems and the ability of guided waves to monitor large structures. However, challenges re-

main in processing high dimensional sensor data and there is a need for accurate and reliable damage detection and monitoring methods especially for composite materials with anisotropic properties and multiple failure modes. In this paper we studied a new multivariate damage monitoring method for Lamb-wave sensing data. A multivariate cumulative sum test statistic was applied to the features extracted with principal components analysis in order to improve the robustness of detection and sensitivity to small damages.

Two case studies were presented using measured sensor data from fatigue loading and impact tests of carbon fiber materials. The monitoring performance of the proposed CUSUM approach was compared with existing Mahalanobis distance based monitoring techniques applied in the health monitoring literature. The results followed our expectation that the existing monitoring methods work reasonably well for relatively large changes in the structural condition, however, supplementing them with a statistic that accumulates information over time can make the monitoring much more sensitive to gradually developing damages. This can enhance the ability to continuously monitor growing damages and react to them by scheduling repair or replacement actions before they reach critical size and result in failure. Fatigue loading data from multiple specimens showed that CUSUM approach can have significantly lower misdetection rates. Possible extensions of this research would include, accommodating for environmental fluctuations in the monitoring method (Cross et al., 2012) and modeling the degradation path as a stochastic process (Lu & Meeker, 1993) in order to make inferences about remaining useful life.

ACKNOWLEDGEMENTS

We thank the NASA Ames Research Center for allowing us to use the fatigue data set in our illustrations.

REFERENCES

- Bogdanoff, J. L., & Kozin, F. (1985). *Probabilistic models of cumulative damage*. New York: John Wiley.
- Crosier, R. (1988). Multivariate generalizations of cumulative sum quality-control schemes. *Technometrics*, 30(3), 291–303.
- Cross, E. J., Manson, G., Worden, K., & Pierce, S. G. (2012). Features for damage detection with insensitivity to environmental and operational variations. *Proceedings of the Royal Society A: Mathematical, Physical and Engineering Science*, 468(2148), 4098–4122.
- Deraemaeker, A., Reynders, E., De Roeck, G., & Kullaa, J. (2008). Vibration-based structural health monitoring using output-only measurements under changing environment. *Mechanical systems and signal processing*, 22(1), 34–56.

- Diamanti, K., Hodgkinson, J. M., & Soutis, C. (2004). Detection of low-velocity impact damage in composite plates using lamb waves. *Structural Health Monitoring*, 3(1), 33–41.
- Gertsbackh, I. B., & Kordonskiy, K. B. (1969). *Models of failure*. New York: Springer-Verlag.
- Giurgiutiu, V. (2005). Tuned lamb wave excitation and detection with piezoelectric wafer active sensors for structural health monitoring. *Journal of intelligent material systems and structures*, 16(4), 291–305.
- Ihn, J. B., & Chang, F. K. (2004). Detection and monitoring of hidden fatigue crack growth using a built-in piezoelectric sensor/actuator network: I. diagnostics. *Smart Materials and Structures*, 13(3), 609.
- Jackson, J. E. (2005). *A user's guide to principal components* (Vol. 587). John Wiley & Sons.
- Kessler, S. S., & Agrawal, P. (2007). Application of pattern recognition for damage classification in composite laminates. In *Proceedings of the 6th international workshop on structural health monitoring, stanford university*.
- Kessler, S. S., Spearing, S. M., & Soutis, C. (2002). Damage detection in composite materials using lamb wave methods. *Smart Materials and Structures*, 11(2), 269.
- Kullaa, J. (2003). Damage detection of the z24 bridge using control charts. *Mechanical Systems and Signal Processing*, 17(1), 163–170.
- Lowry, C. A., & Montgomery, D. C. (1995). A review of multivariate control charts. *IIE transactions*, 27(6), 800–810.
- Lu, C. J., & Meeker, W. O. (1993). Using degradation measures to estimate a time-to-failure distribution. *Technometrics*, 35(2), 161–174.
- MacGregor, J. F., & Kourti, T. (1995). Statistical process control of multivariate processes. *Control Engineering Practice*, 3(3), 403–414.
- Montgomery, D. C. (2007). *Introduction to statistical quality control*. John Wiley & Sons.
- Mujica, L. E., Rodellar, J., Fernandez, A., & Guemes, A. (2010). Q-statistic and t2-statistic pca-based measures for damage assessment in structures. *Structural Health Monitoring*, 1475921710388972.
- Pavlopoulou, S., Worden, K., & Soutis, C. (2013). Structural health monitoring and damage prognosis in composite repaired structures through the excitation of guided ultrasonic waves. In *Spie smart structures and materials+ non-destructive evaluation and health monitoring* (pp. 869504–869504).
- Pignatiello, J. J., & Runger, G. C. (1990). Comparisons of multivariate cusum charts. *Journal of quality technology*, 22(3), 173–186.
- Pullin, R., Eaton, M. J., Hensman, J. J., Holford, K. M., Worden, K., & Evans, S. L. (2008). A principal component analysis of acoustic emission signals from a landing gear component. *Applied Mechanics and Materials*, 13, 41–47.
- Raghavan, A., & Cesnik, C. (2007). Review of guided-wave structural health monitoring. *Shock and Vibration Digest*, 39(2), 91–116.
- Saxena, A., Goebel, K., Larrosa, C. C., & Chang, F. K. (2015). *CFRP Composites dataset, NASA Ames Prognostics Data Repository*. <http://ti.arc.nasa.gov/project/prognostic-data-repository>. Accessed Jan 18, 2015. NASA Ames, Moffett Field, CA.
- Sohn, H., Czarnecki, J. A., & Farrar, C. R. (2000). Structural health monitoring using statistical process control. *Journal of Structural Engineering*, 126(11), 1356–1363.
- Su, Z., Ye, L., & Lu, Y. (2006). Guided lamb waves for identification of damage in composite structures: A review. *Journal of sound and vibration*, 295(3), 753–780.
- Viktorov, I. A. (1967). *Rayleigh and lamb waves. physical theory and applications*. Plenum Press.
- Wang, W. (2000). A model to determine the optimal critical level and the monitoring intervals in condition-based maintenance. *International Journal of Production Research*, 38(6), 1425–1436.
- Woodall, W. H., & Ncube, M. M. (1985). Multivariate cusum quality-control procedures. *Technometrics*, 27(3), 285–292.
- Worden, K., Manson, G., & Fieller, N. R. J. (2000). Damage detection using outlier analysis. *Journal of Sound and Vibration*, 229(3), 647–667.